Shear band melting and serrated flow in metallic glasses

K. Georgarakis, M. Aljerf, Y. Li, A. LeMoulec, F. Charlot et al.

Related Articles

Nonlinear viscoelasticity of freestanding and polymer-anchored vertically aligned carbon nanotube foams
J. Appl. Phys. 111, 074314 (2012)

Defect-induced solid state amorphization of molecular crystals
J. Appl. Phys. 111, 073505 (2012)

Notable internal thermal effect on the yielding of metallic glasses
Appl. Phys. Lett. 100, 141904 (2012)

Sheared polymer glass and the question of mechanical rejuvenation
J. Chem. Phys. 136, 124907 (2012)

Growth stress in SiO2 during oxidation of SiC fibers
J. Appl. Phys. 111, 063527 (2012)

Additional information on Appl. Phys. Lett.

Journal Homepage: http://apl.aip.org/

Journal Information: http://apl.aip.org/about/about_the_journal

Top downloads: http://apl.aip.org/features/most_downloaded

Information for Authors: http://apl.aip.org/authors

Shear band melting and serrated flow in metallic glasses

K. Georgarakis,[1] M. Aljerf,[1] Y. Li,[1] A. LeMoulec,[1] F. Charlot,[1] A. R. Yavari,[1,a)]
K. Chornokhvostenko,[2] E. Tabachnikova,[2] G. A. Evangelakis,[3] D. B. Miracle,[4] A. L. Greer,[5]
and T. Zhang[6]

[1]*Euronano, SIMaP-CNRS, Institut National Polytechnique de Grenoble, BP 75, Saint Matrin d'Heres campus 38402, France*
[2]*Kharkiv Polytechnic Institute, 61002 Ukraine*
[3]*Department of Physics, University of Ioannina, Ioannina 45110, Greece*
[4]*Materials and Manufacturing Directorate, Air Force Research Laboratory, Wright-Patterson Air Force Base, Ohio 45433, USA*
[5]*Department of Materials Science and Metallurgy, Cambridge University, CB2 3QZ United Kingdom*
[6]*Beijing University of Aeronautics and Astronautics, Beijing 100083, People's Republic of China*

Scanning electron microscopy observations of shear steps on Zr-based bulk metallic glasses show direct evidence of shear band melting due to heat generated by elastic energy release. The estimated range of attained temperatures and the observed morphologies are consistent with shear steps forming at a subsonic speed limited by a required redistribution of local microscopic stresses. The calculations indicate that a 0.2 μm layer melts in the vicinity of a shear band forming a 1 μm shear step. The plastic part of the stress strain curve is serrated but a majority of shear events are not associated to serrations. © *2008 American Institute of Physics*. [DOI: 10.1063/1.2956666]

Metallic glasses[1] exhibit a perfectly elastic strain range ε_{el} of about 2% which, depending on their elastic moduli, may require applied stresses as high as 5 GPa or more[2] and allows them to store record amounts of elastic energy as springs, pressure gauges, microgears, and impact rebound enhancement parts in sports equipment.

In the absence of dislocations and crystallographic slip, plastic deformation in metallic glasses occurs heterogeneously in shear bands that are thin layers of material initially only $\sim$10 nm thick[3] at approximately 45° to the stress axis.

With $\varepsilon_{el} \approx 2\%$, the total stored elastic energy per unit volume H_{max} prior to plastic yielding is

$$H_{max} \approx \left(\tfrac{1}{2}\right)\sigma^{\circ}\varepsilon_{el} = \left(\tfrac{1}{2}\right)E\varepsilon_{el}^2, \qquad (1)$$

where σ° is the maximum applied elastic stress and E is the Young modulus.

For the commonly used Zr-based metallic glasses $E \approx 10^{11}$ Pa, leading to maximum stored elastic energies of $H_{max} \lesssim 20$ J/cm^3. With volume specific heat $c_p \approx 3$ J/K cm^3, when such elastic energy is homogeneously relaxed, as upon removal of applied stress in hydrostatic pressure geometries, its total conversion to heat does not lead to large temperature increases, with $\Delta T_{max} \approx H_{max}/c_p < 7$ K. However, if this elastic energy were to be converted to heat by heterogeneous deformation within very thin shear bands, simple calculations show that temperatures would reach thousands of degrees and fracture surfaces of metallic glasses indeed bear vein patterns and dropletlike features indicative of melting.[4,5]

Lewandowski and Greer[6] reported temperature increases ΔT of the order of 1000 K in the thermal diffusion zone near shear bands in bulk metallic glasses (BMGs) using a "fusible" coating method. Others also reported very high temperatures attained in or near shear bands for specimens tested in compression and in tension.[7] Nanocrystals[8–12] have been detected in or around shear bands, the nanocrystal formation and growth being other indications of heating due to shear.

In this work we present direct experimental evidence of melting due to shear using a field emission gun (FEG)-equiped scanning electron microscope (SEM).

Shear steps formed during compression at strain rates 10^{-4} s^{-1} were examined on deformed cylindrical BMG specimens of composition Zr$_{62}$Cu$_{15.5}$Ni$_{12.5}$Al$_{10}$ previously referred to as S3 (Ref. 13) and Zr$_{62}$Cu$_{15.5}$Ni$_{12.5}$Al$_{10}$ with 1 at % Y addition using SEM. The reported unlimited plastic deformability in compression[13] of Zr$_{62}$Cu$_{15.5}$Ni$_{12.5}$Al$_{10}$ BMGs was not observed. Each of many such samples tested in compression breaking after a few percent plastic deformation but this extent of deformation is appropriate for examination of individual shear bands.

Figure 1 shows a shear step on the surface of a Zr$_{62}$Cu$_{15.5}$Ni$_{12.5}$Al$_{10}$ BMG. It is a rather featureless step having formed meniscus with the upper part of the specimen indicating that the entire width of the step of about 5 μm melted at some point but this type of feature is rather rare on shear steps.

Figure 2 shows a shear step on a BMG cylinder Zr$_{62}$Cu$_{15.5}$Ni$_{12.5}$Al$_{10}$ with 1 at % Y addition. The waves on
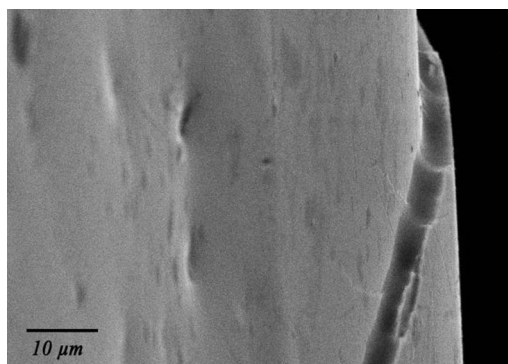

FIG. 1. A rather featureless shear step having formed meniscus with the upper part of the BMG specimen.
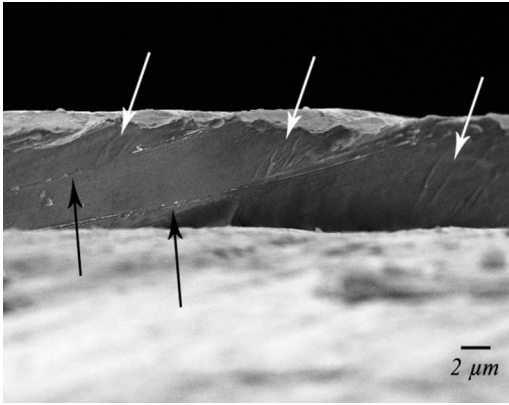
FIG. 2. Waves (white arrows) on a shear step on BMG surface indicating liquid stages in its history. The waves do not cross lines (black arrows) on the surface indicating that the step formed in several stages.

the step surface indicate liquid stages in its history (white arrows). Interestingly, lines are visible on the surface (black arrows) and the wavy shapes do not cross these lines. The significance of these lines is not known but they seem to indicate that the shear step was formed in several stages. Ample evidence of welding and meniscus forming at the bottom of steps was observed as seen in the example of Fig. 3 ($Zr_{62}Cu_{15.5}Ni_{12.5}Al_{10}$ plus 1 at % Y) where U-shaped meniscus are seen at the step base, indicating viscous behavior and high temperatures. The meniscus has $1-2$ μm radius of curvature, two orders of magnitude larger than the presumed thickness of the shear band itself, often[3] about $10-50$ nm.

While melting (Fig. 1), successively melted zones (Fig. 2), tearing and welding and meniscus formation (Fig. 3) are observed on shear steps, step size varies around the specimen and different features may be observed on the same step at different locations.

At room temperature, the plastic region of stress-strain curves of Zr-based metallic glasses are not monotonous and show small load or stress drops $\Delta\sigma$ referred to as "serrations" as in the Portevin–Le Chatelier effect due to dislocation-solute atmosphere interactions in crystalline materials.[14] However, metallic glasses do not deform by dislocation glide and the origin of these serrations is as yet unknown.

In the present tests, serrations correspond to stress drops $\Delta\sigma$ of the order of 1% of the applied (yield) stress $\sigma°$ (see Fig. 4). The elastic strain must also drop by $\Delta\varepsilon_{el}$ as per Hook's law $(\Delta\sigma/\sigma°)=(\Delta\varepsilon_{el}/\varepsilon_{el}°)$ such that the stress drop would correspond to an elastic energy release of
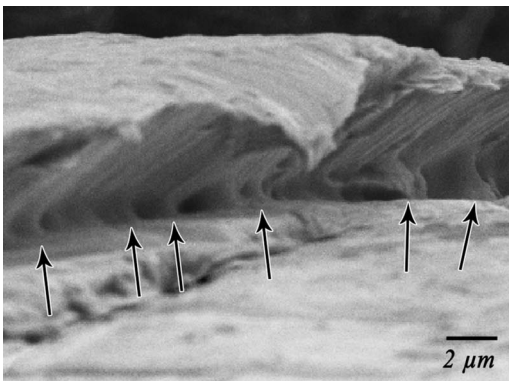

FIG. 3. Arrows show U-shaped meniscus locations at the step bottom indicating viscous behavior and high temperatures at the end of the shear event.
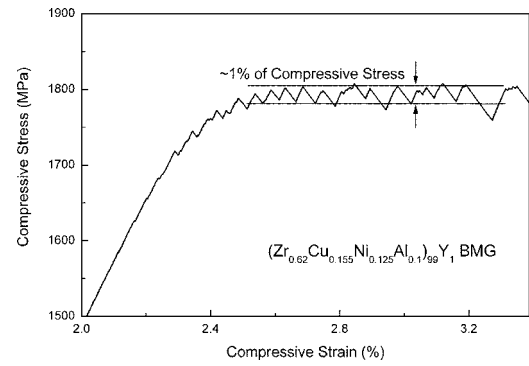

FIG. 4. Serrations on a stress-strain curve of a Zr-based BMG.

$$\Delta H_{max} \approx \left(\tfrac{1}{2}\right)E\varepsilon_{el}°^2 - \left(\tfrac{1}{2}\right)E(\varepsilon_{el}° - \Delta\varepsilon_{el})^2 \approx E\varepsilon_{el}°\Delta\varepsilon_{el}$$
$$- \left(\tfrac{1}{2}\right)E\Delta\varepsilon_{el}^2 \approx E\varepsilon_{el}°\Delta\varepsilon_{el} \approx E\varepsilon_{el}°^2(\Delta\sigma/\sigma°), \quad (2)$$

where $\left(\tfrac{1}{2}\right)E\Delta\varepsilon_{el}^2 \ll E\varepsilon_{el}°\Delta\varepsilon_{el}$ has been neglected and $\Delta H_{max}/H_{max} \approx 2$ $(\Delta\sigma/\sigma°)$ or about 2%. With a specimen length L of 4 mm, $\Delta\varepsilon_{el} \approx 1\%$ $\varepsilon_{el}° \approx 2\times10^{-4}$ corresponds to a shear step of the order of 1 μm in size. In the calculations that follow, we will use three different approximations for the time τ_{shear} associated with a shear event that results in a step or increment of step 1 μm in size whether associated with a serration or not.

Assuming that the shear band operates as a zero-thickness planar heat source of constant flux q_s, the temperature at a distance x_{th} from the shear band after time $t=\tau_{shear}$ of operation can be found from the one-dimensional profile.[15]

$$T(x,t) = T_0 + \frac{q_s}{2c_p \cdot \alpha}\left(\sqrt{\frac{4\alpha t}{\pi}}e^{-x^2/4\alpha t} - x\,\mathrm{erfc}\left(\frac{x}{\sqrt{4\alpha t}}\right)\right),$$
$$(3)$$

where T_0 is the initial temperature, c_p is the volumetric specific heat, $\alpha \approx 2\cdot10$ cm^2/s is the thermal diffusivity, and erfc$=1-$erf is the complementary error function.

The assumption of the constant heat flux q_s is debatable as it is not known how a shear band starts then stops operating and how the extent of elastic energy release depends on the temperatures attained during the deformation. Nevertheless, we will consider three limiting cases using Eq. (3) for three different characteristic times τ_{shear} for the elastic energy release corresponding to three values of the heat flux $q_s \approx \Delta H_{max}\cdot L/\tau_{shear}$ where L is the specimen length of 4 mm:

(1) $\tau_{shear}=\tau_1=\tau_{step}$ (d_{step}) for the formation of a shear step of size d_{step} at the speed of sound v_s.
(2) $\tau_{shear}\approx\tau_2=\tau_{sound}$ (x_{sound}) for the elastic propagation of a stress-redistribution wave in front of the shear band to a distance x_{sound} (see below).
(3) $\tau_{shear}\approx\tau_3=\tau_{serr}$ of one serration stress drop time[16–18] of the order of 0.1 s.

For all three cases we consider the elastic energy of Eq. (2), corresponding to the formation of 1 μm size step: $\Delta H_{max}\approx E\cdot\varepsilon_{el}°^2\cdot(\Delta\sigma°/\sigma)\approx 0.02H_{max}$ and which is about 0.4 J/cm^3.

In the first case, with heating due to elastic energy release ΔH_{max} occurring during shear producing a step d_{step}
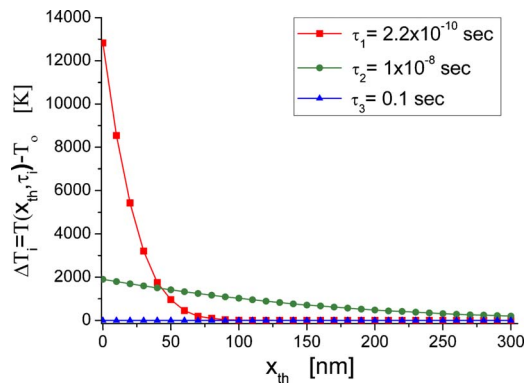
FIG. 5. (Color online) Calculated temperature rise vs distance x_{th} away from the shear band during formation of a micron-size shear step. When the step is required to form under positive local stress conditions ($\tau_{shear} \approx \tau_2 \approx 10$ ns), a thermal diffusion layer $2x_{th}$ of approximately 0.2 μm is found to heat to $T > 1300$ K which melts all Zr-based metallic glasses.

≈ 1 μm at the speed of sound $v_s \approx 4.5 \times 10^5$ cm/s, ΔH_{max} would be released quasiadiabatically during the time $\tau_{shear} \approx d_{step}/v_s \approx 2.2 \times 10^{-10}$ s or 0.2 ns.

For the second case, let us consider more closely the formation of a shear step d_{step} in uniaxial compression at the speed of sound v_s. As d_{step} forms at approximately 45° angle to the specimen length L, the sample length decreases by $d_{step}/\sqrt{2}$. If d_{step} were to come out at the speed of sound v_s, the specimen length near the shear band at distances x_{sound} simultaneously reachable by the consequent acoustic relaxation wave ($x_{sound} \approx d_{step}$) would come under colossal elastic tension $\varepsilon_{el} \approx -1/\sqrt{2}$ opposite to and far larger in magnitude than the compressive applied elastic strain. The corresponding local tensile stress field would make it impossible for the step to continue. As the shear step d_{step} forms, a stress-redistribution layer x_{sound} is required in the vicinity of the shear band such that it remains under a nonzero applied stress. For this to occur, stress redistribution is required in a layer $x_{sound} \approx d_{step}/\varepsilon_{el}^{\circ}\sqrt{2}$. Since this stress redistribution must be established by a traveling transversal sound wave at velocity v_s, it requires a time $\tau_{shear} \approx d_{step}/\varepsilon_{el} \sqrt{2} \cdot v_s \approx 10^{-8}$ s for $d_{step} \approx 1$ μm.

Instrumented uniaxial compression testing with a strain guage placed on the sample acquiring data points at 200–1000 Hz can trace the kinetics of the stress drops or serrations and reveal that a stress drop occurs over a time[16–18] of the order of $\tau_{serr} \approx 0.1$ s. Thus for the third case we take $\tau_{shear} \approx \tau_3 \approx \tau_{serr} \approx 0.1$ s.

Figure 5 plots the resulting temperature rise versus distance x_{th} away from the center plane of the band (or the heat source) after the three different characteristic shear times τ_{shear} for the formation of a micron-size shear step.

As expected, the assumption of a shear step forming at the speed of sound ($\tau_{shear} \approx \tau_1 \approx 0.2$ ns) leads to unrealistically high values of temperature.

When the step is required to form under realistic positive stress condition ($\tau_{shear} \approx \tau_2 \approx 10$ ns), peak temperature rise in a band 10 nm wide is seen to be between 1900 and 2000 K and a thermal diffusion layer $2x_{th}$ of approximately 0.2 μm is heated to $T > 1300$ K which melts all Zr-based BMGs. All together, a $2x_{th}$ about 0.3 μm thick reaches 1000 K and a 0.4 μm thick layer reaches the glass transition near 750 K. These thermal diffusion layers are of the same order of magnitude as those needed to explain the microscopic morpholo-

gies on shear steps of the size used in the calculation (1 μm).

When the step is assumed to form at the slow speed of the stress serration drop ($\tau_{shear} \approx \tau_3 \approx 0.1$ s), the shear band does not heat up significantly. This is in contradiction with clear evidence for melting and meniscus forming on shear steps as presented in the SEM pictures and indicates that serration stress drop times are not the same as those of shear step formation. Indeed, if we sum the total strain $\Sigma\Delta\varepsilon_{serr}$ associated with all individual stress drops (on the average $\Delta\varepsilon_{serr} = (\Delta\sigma/\sigma^{\circ})$ $\varepsilon_{el}^{\circ} \approx 2 \times 10^{-4}$/serration) in Fig. 4 occurring during an interval $\Delta\varepsilon_{plastic}$ of the macroscopic stress-strain curve, we find that $\Sigma\Delta\varepsilon_{serr} \ll \Delta\varepsilon_{plastic}$ such that a majority of the plastic deformation and the shear steps that result from it are not associated to the serrations. In addition, serrations disappear at low temperatures and/or high strain rates[19] while shear bands and shear step formation continue to be the mechanism of deformation.

In conclusion, SEM observations of shear steps on deformed BMGs show direct evidence of melting as expected from elastic energy release in form of heat during shear deformation. Shear steps appeared mostly to have formed in successive increments. The estimated range of attained temperatures and the observed morphologies are consistent with shear steps forming at subsonic speed as required by a local redistribution of microscopic stresses and the maintenance of a nonzero positive local applied stess field at the operating shear band. Stress serrations or load drops observed on stress-strain curves, depending on the temperature and strain rate, are not associated with individual shear events.

[1] W. L. Johnson and K. Samwer, Phys. Rev. Lett. **95**, 195501 (2005).
[2] A. Inoue, B. Shen, H. Koshiba, H. Kato, and A. R. Yavari, Nat. Mater. **2**, 661 (2003).
[3] Y. Zhang and A. L. Greer, Appl. Phys. Lett. **89**, 071907 (2006).
[4] C. A. Pampillo, J. Mater. Sci. **10**, 1194 (1975).
[5] C. J. Gilbert, J. W. Ager, III, V. Schroeder, R. O. Ritchie, J. P. Lloyd, and J. R. Graham, Appl. Phys. Lett. **74**, 3809 (1999).
[6] J. J. Lewandowski and A. L. Greer, Nat. Mater. **5**, 15 (2006).
[7] B. Yang, P. K. Liaw, G. Wang, M. Morrison, C. T. Liu, R. A. Buchanan, and Y. Yokoyama, IEEE Trans. Reliab. **12**, 1265 (2004).
[8] A. R. Yavari, J. J. Lewandowski, and J. Eckert, Mater. Res. Bull. **32**, 8 (2007).
[9] K. Hajlaoui, A. R. Yavari, B. Doisneau, A. LeMoulec, G. Vaughan, A. L. Greer, A. Inoue, and A. Kvick, Scr. Mater. **54**, 1829 (2006).
[10] K. Hajlaoui, B. Doisneau, A. R. Yavari, W. Zhang, G. Vaughan, A. Inoue, and A. L. Greer, Mater. Sci. Eng., A **449**, 105 (2007).
[11] K. Wang, T. Fujita, Y. Q. Zeng, N. Nishiyama, A. Inoue, and M. W. Chen, Acta Mater. **56**, 2834 (2008).
[12] T. Zhang and H. Men, J. Alloys, J. Alloys Compd. **10**, 434 (2007).
[13] Y. H. Liu, G. Wang, R. J. Wang, D. Q. Zhao, M. X. Pan, and W. H. Wang, Science **315**, 1385 (2007).
[14] A. H. Cottrell, Philos. Mag. **44**, 829 (1953).
[15] D. R. Pitts and L. E. Sissom, *1000 Solved Problems in Heat Transfer* (McGraw-Hill, New York, 1991).
[16] F. Dalla Torre, A. Dubach, M. Siegrist, and J. Löffler, Appl. Phys. Lett. **89**, 091918 (2006).
[17] W. J. Wright, R. B. Schwarz, and W. D. Nix, Mater. Sci. Eng., A **319**, 229 (2001).
[18] F. Dalla Torre, A. Dubach, A. Nelson, and J. Löffler, Mater. Trans., JIM **48**, 1774 (2007).
[19] W. H. Jiang, F. Jiang, F. X. Liu, H. Choo, and P. K. Liaw, Appl. Phys. Lett. **89**, 261909 (2006).